REVISTA DE METALURGIA, 47 (2)
MARZO-ABRIL, 126-137, 2011
ISSN: 0034-8570
eISSN: 1988-4222
doi: 10.3989/revmetalmadrid.1003

Oxidation behaviour at 1123 K of AISI 304-Ni/Al-Al_2O_3/TiO_2 multilayer system deposited by flame spray(•)

K.A. Habib*, J.J. Saura*, C. Ferrer**, M.S. Damra* and I. Cervera*

Abstract

The oxidation behaviour of alumina/titania (97/3, 87/13 and 60/40) ceramic coatings using a Ni-Al coupling layer was studied in a thermobalance. Both layers were deposited on an AISI 304 stainless steel base metal by the flame spray technique. The coated steel was heated from room temperature to 1,123 K at 40 K min^{-1}, oxidized in air for 50 h, and then cooled to room temperature at 40 K min^{-1}. The mass gain was mainly attributed to the oxidation of Ni-Al coupling layer. Kinetic laws, $\Delta W \cdot S^{-1}$ ($mg.mm^{-2}$) vs. time (hours) were close to a parabolic plot for each sample. Surface composition of ceramic top layer and the cross section of multilayer system were analysed using a wide range of experimental techniques including Scanning Electron Microscopy (SEM), equipped with a link energy dispersive X-Ray spectroscopy (EDX) and X-Ray diffraction (XRD) before and after the oxidation process. Coatings 97/3 and 87/13 presented a stable structure after flame spray deposition and they did not evolve with the oxidation process, while most of the 60/40 coating changed to a metastable structure after deposition and to a more stable structure after oxidation with high micro-cracks content. SEM and EDX microanalysis of the cross-sections showed that significant oxidation and a weak intergranular precipitation had been produced in the coupling layer and on the stainless steel base metal, respectively.

Keywords

AISI 304; Coupling layer Ni-Al; Alumina-titania layers; Flame spray; High temperature oxidation.

Oxidación a 1123 K de sistemas multicapa AISI 304-Ni/Al-Al_2O_3/TiO_2 depositados mediante proyección por llama

Resumen

El comportamiento a oxidación de recubrimientos cerámicos alúmina/titania (97/3, 87/13, 60/40) usando una capa de anclaje Ni-Al se ha estudiado mediante una termobalanza. Ambas capas se han depositado sobre un acero inoxidable AISI 304 utilizando la técnica de proyección llama (FS). El acero recubierto se ha calentado desde la temperatura ambiente hasta 1.123 K a 40 K min^{-1}, se ha oxidado al aire durante 50 h, y luego se ha enfriado hasta la temperatura ambiente a 40 K min^{-1}. La ganancia en masa se atribuye a la oxidación de la capa de enganche Ni-Al. La cinética $\Delta W \cdot S^{-1}$ ($mg.mm^{-2}$) vs. tiempo (horas) se ha ajustado a una ley parabólica para todas las muestras. La composición superficial de la capa cerámica y la sección transversal del sistema multicapa se han analizado mediante las técnicas de Microscopía Electrónica de Barrido (SEM), Espectroscopia de Energías Dispersivas de Rayos X (EDX), Difracción de Rayos X (XRD) antes y después del proceso de oxidación. Los recubrimientos 97/3 y 87/13 han presentado una estructura estable tras el proceso de deposición por proyección por llama y esta estructura tampoco ha evolucionado después de la oxidación, mientras la mayor parte del recubrimiento 60/40 ha cambiado a una estructura metaestable después la deposición y finalmente ha evolucionado a una estructura más estable después de la oxidación con alto contenido de microagrietamiento. El microanálisis mediante SEM y EDX de las secciones transversales han mostrado una oxidación significativa en la capa de enganche y una débil precipitación intergranular en el material base AISI 304.

Palabras clave

AISI 304; Capa de anclaje Ni-Al; Capas alúmina-titania; Proyección llama; Oxidación alta temperatura.

1. INTRODUCTION

Alumina/titania coatings are excellent candidates for providing protection against abrasive wear and resistance to galvanic and moderate temperature oxidation. Such coatings are required for electrical insulation and anti-wear applications where galvanic corrosion must be avoided. Examples include their use in solar dynamic (SD) space power systems, heat receiver interior surfaces, protective coatings

(•) Trabajo recibido el día 21 de Enero de 2010 y aceptado en su forma final del día 27 de Septiembre 2010.
* Departamento de Ingeniería de Sistemas Industriales y Diseño, Universitat Jaume I. 12071 Castellón, Spain, E-mail: *razzaq@esid.uji.es.*
** Departamento de Ing. Mecánica y de Materiales, UPV, Valencia, Spain.

for sleeve shafts, thermocouple jackets, electrical insulators, pump shafts and in any other application where it is necessary to combine high resistance to wear, a low friction coefficient and moderate service temperatures[1-4]. These coatings are usually applied by using plasma spray (PS), high-velocity oxygen fuel (HVOF) and flame spray (FS) techniques[5 y 6].

The flame spray deposition technique has some disadvantages compared to the PS or HVOF methods, including a bigger grain size microstructure, pores size and crack length. However, it also has certain advantages, such as being more economical, easier to handle and more adaptable to manufacturing processes with short series or recovery of pieces. Flame spray was the first thermal spray process developed (c.1910). Modern torches have changed and the high particle velocities are now in the range of 200-300 m/s. Oxyacetylene torches use acetylene as the main fuel in combination with oxygen to generate high combustion temperatures and a maximum particle temperature of around 3,000 °C.

High temperature reached during thermal spray processes is considered to be necessary to melt the ceramic powder particles. The coatings can present pores and cracks. In recent years there has been a tendency to improve the mechanical properties and tribological behaviour by employing fine-grained structures (i.e. nanomaterials), although the deposition guns have a strong influence, like the coatings deposited by HVOF are significantly harder, tougher and with higher abrasion resistance than the PS and FS [7].

Ceramic coatings are generally suitable for high temperature oxidation due to the α-alumina content[8-10], but an increase in the service temperature leads to more structural stability, which could reduce its oxidation resistance.

Thermally sprayed alumina protects the substrate by obstructing oxygen and aluminium diffusion, thus hindering fast-growing oxide formation, such as Cr_2O_3, NiO, spinels, etc. The main feature of alumina-former alloys and alumina coatings is their resistance to thermal cycles and high temperature oxidation[11 and 12].

Alumina/titania coatings obtained by thermal spray techniques are widely used to prevent against relatively low temperature abrasive wear[13-15]. However, at moderate temperature the oxidation and abrasive wear resistance of these porous ceramic coatings can be reduced[16].

Several studies[17-24] highlight that, at high temperature in the oxidation environment, chromia-forming alloys such as austenitic stainless steels present an initial protect and adherent oxide growth leading mainly to chromia formation. Cr_2O_3 scales can be volatilized at approximately 1,173 K, or even at 1,073-1,123 K, depending on the oxygen partial pressure in the atmosphere. Some authors consider 1,023 K to be a suitable temperature to obtain optimum performance in this type of stainless steel[25]. The oxidation in air at 1,273 K shows that the scale formed is composed of two subscales; internal adherent and external spalled subscales, chromia appears to be slightly present in the adherent subscale and two spinels $Mn_{1.5}Cr_{1.5}O_4$ and $FeCr_2O_4$ as well as hematite Fe_2O_3 in the external spalled subscale[26].

Due to its good resistance to high temperature oxidation, austenitic AISI 304 stainless steel was selected as the base metal because the ceramics coating Al_2O_3/TiO_2 are usually porous and can fail in this application. Alumina/titania coatings are good candidates for providing resistance against the abrasive wear of these types of steels[27 y 28], but if the multilayer system stainless steel-Ni/Al-Al_2O_3/TiO_2 coatings reaches temperatures higher than 1,023K, even if just for short times, it may produce degradation of the stainless steel.

According to some authors the Al_2O_3/TiO_2 oxidation is generally studied at temperatures lower than 1,123 K, but for some applications such as industrial ovens and superheated tubes in biomass plants, it is interesting to test these coatings in a higher temperature range in order to analyze the composition of phases formed at testing temperature by XRD, XRD, SEM and EDX. The aim of the present work is then to analyse the oxidation behaviour at 1,123 K of multilayer system using three ceramic finish coatings, with different ratios of alumina/titania, applied under optimized working conditions, and to explain the failure reasons of AISI 304- Ni/Al- Al_2O_3/TiO_2 system.

2. EXPERIMENTAL PROCEDURES

The bulk composition of AISI 304 stainless steel used as base metal is presented in table I.

AISI 304 stainless steel plates of 20 × 10 × 1.2 mm^3 were used as substrates. All sides of these samples were ground to SIC # 600 and grit-blasted with corundum particle of 99.6 wt % of purity and 0.53 mm of mean particle size, using an air pressure of 0.4 MPa, incidence angle of ~ 45° and a gun-to-substrate distance of 130 mm. The surface was then cleaned and degreased using acetone within an ultrasonic bath. The average surface roughness of 5.1 ± 0.5 μm and the mean roughness depth (defined as the vertical distance between the highest peak and deepest valley) of 28.3 ± 2.4 μm were measured using a profilometer (Perthometer M1, Mahr GMBH, Germany).

Table I. Chemical composition of austenitic AISI 304 stainless steel (wt %)

Tabla I. Composición química del acero inoxidable AISI 304 (% peso)

Cr	Ni	Mn	Cu	Co	Mo	Si	C	P	S	N	V	Nb	Ti
18.21	8.18	1.51	0.30	0.12	0.21	0.42	0.065	0.032	0.002	0.0389	0.083	0.009	0.003

Table II shows the spray parameters for the coupling layer and the ceramic coatings[29].

Two different powders were deposited on all the sample faces by a CDS-8000 flame spray gun: one consisted of Rototec 51000, a commercial powder with 88.1 % Ni, 6.04 % Al, 5.25 % Mo, 0.36 % Fe and 0.22 % Cr by weight and a grain size of 40 - 113 μm, which operates as a coupling layer; the second was a ceramic finishing layer (Metaceram 28020, 28030, 28060), with three different compositions containing 97/3, 87/13 and 60/40 alumina/titania respectively and a grain size smaller than 60 μm. All these products were supplied by Castolin Eutectic.

In order to prepare the top surface of the alumina/titania ceramic coatings, samples were polished using three sequential steps, namely 6, 3, and 1 μm grade diamond lapping, in that order, and were ultrasonically cleaned out with acetone for 15 minutes.

Samples were heated in a thermobalance (TGA 92-16, Setaram) with synthetic air (1 bar pressure) from room temperature to 1,123 K at a rate of 40 $K \cdot min^{-1}$. They were maintained at that temperature for 50 h and then cooled to room temperature at 40 $K \cdot min^{-1}$.

The volume fraction of the different oxidize phases was calculated using quantitative image analysis (Omnimet Advantage Image Analyzer and Buehler Image Analysis System).

3. RESULTS

3.1. Thermogravimetry

Table III summarizes the relative mass gain rate of the multilayer system after 50 h of exposure in a synthetic air atmosphere during isothermal oxidizing at 1,123 K.

The plot of mass gain per unit surface area for isothermal holding ΔW/S against oxidation time (t) follows a parabolic law in accordance with the equation:

$$\Delta W/S = K_p\, t^{0.5} \qquad (1)$$

where K_p is the isothermal parabolic rate constant.

Figure 1 shows that as the titania content increases, the oxidation resistance of the multilayer system is clearly reduced. Furthermore AISI 304

Table II. Thermal spray parameters

Tabla II. Parámetros de proyección térmica

Sample	Gun velocity (mm/seg)	Sprayed alloy	Preheating stroke Nº	Spray stroke Nº	Powder flow (g/min)	Spraying distance (mm)	Acetylene pressure (bar)	Oxygen press. (bar)	Compressed air (bar)	Flame type	Thickness (μm)
97/3	67.5	Rototec 51000	1	1	3	150	0.7	3	1.5	Neutral	170
87/13	67.5	Rototec 51000	1	1	3	150	0.7	3	1.5	Neutral	165
60/40	67.5	Rototec 51000	1	1	3	150	0.7	3	1.5	Neutral	180
97/3	67.5	28020	0	5	1.1	85	0.8	4	3	Neutral	490
87/13	67.5	28030	0	5	2	100	0.8	4	3	Neutral	485
60/40	67.5	28060	0	5	2.06	100	0.8	4	3	Neutral	410

Table III. Mass gain/unit area of multilayer systems, 50 h at 1,123 K

Tabla III. Ganancia en masa/unidad de área de sistemas multicapa, 50 h a 1.123 K

Material	ΔW/S (mg/mm^2)	K_p (gr)^2/ (cm)^4·(s)
AISI 304	0.0024	$8{,}272\cdot10^{-7}$
97/3	0.0326	$8{,}949\cdot10^{-6}$
87/13	0.0403	$1{,}110\cdot10^{-5}$
60/40	0.0459	$1{,}219\cdot10^{-5}$

stainless steel exhibits lower oxidation rates due to the formation an adherent and continuous layer of Cr_2O_3 or $(Cr, Fe)_2O_3$ [30].

3.2. X-Ray Diffraction

The results of XRD analysis of the initial powder and as sprayed of the three ceramic coatings are shown in figure 2.

Al_2O_3/TiO_2 coatings exposed to 1,123 K for 50 h form a stabilized microstructure; thus the as-sprayed coating of 97/3 has a mostly rhombohedral α-alumina structure with a very low proportion of δ-alumina (cubic) and δ-alumina (tetragonal). Therefore, the total disappearance of δ-alumina and the typical peaks of α and γ stable alumina were detected after the oxidation process, as seen in figure 3 a). Coating 87/13 presents the characteristic peaks of α-alumina and titania. Such phases have a high-stability structure, and no appreciable component modifications were detected after the oxidation process, as shown in figure 3 b). Finally, coating 60/40, with an orthorhombic Al_2TiO_5 structure (pseudobrookita type), changes to more stable phases, such as titania and α-alumina, and reduces the Al_2TiO_5 proportion (see figure 3 c)).

3.3. Scanning Electron Microscope

Surface observation

The surface of 97/3 sample is mostly covered by alumina particles and the volume fraction of the pores in the top ceramic layer is relatively high (53 %) due to a considerable amount of partially melted particles (melting temperature 2,313 K). Titania particles (melting temperature 2,103 K) are melted

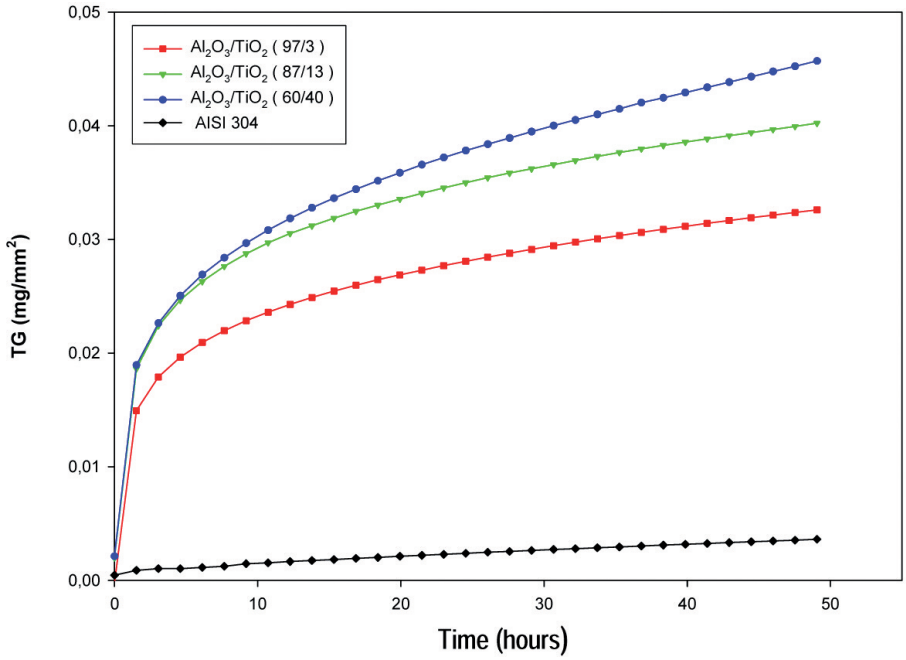

Figure1. Comparison of AISI 304 base metal and ceramic coating layers Al_2O_3/TiO_2 during air oxidation at 1123 K, for 50 h.

Figura 1. Comparación del metal base AISI 304 y los recubrimientos cerámicos Al_2O_3/TiO_2 durante la oxidación en aire a 1123 K durante 50 h.

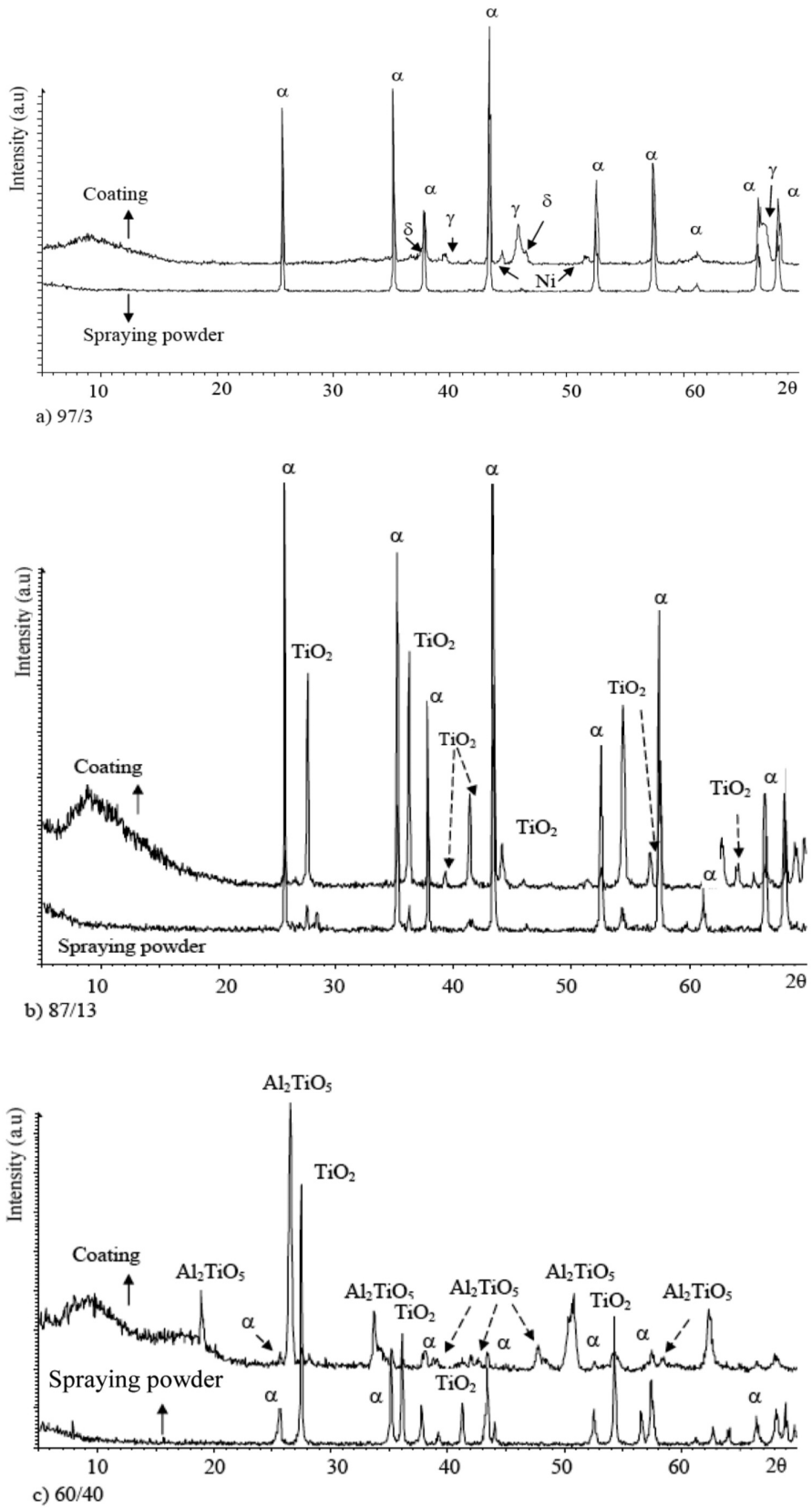

Figure 2. XRD diffraction patterns of alumina-titania; a) 97/3, b) 87/13, c) 60/40 spraying powders and coatings.

Figura 2. Espectros de difracción de polvos de proyección alúmina-titania; a) 97/3, b) 87/13, c) 60/40 y recubrimientos.

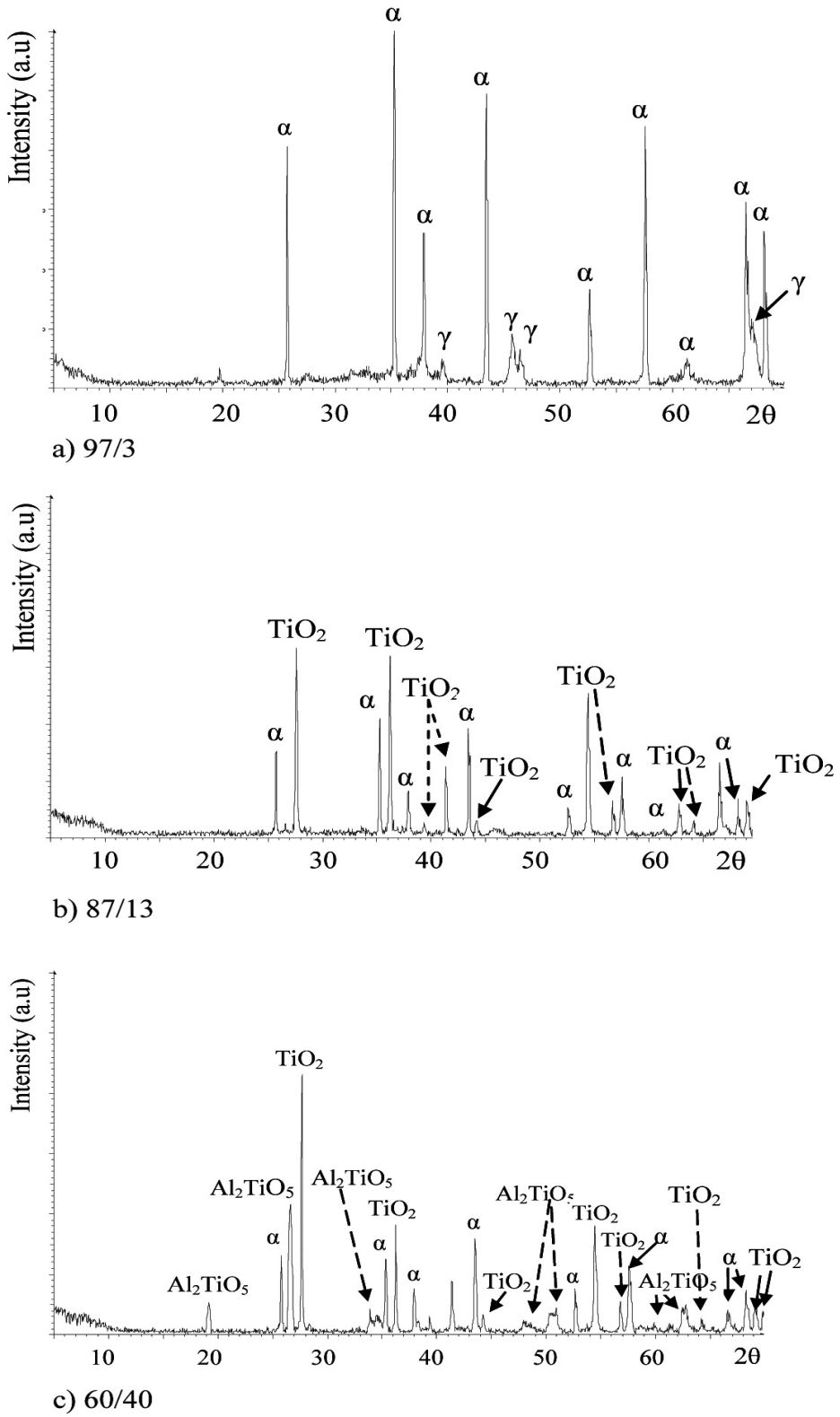

Figure 3. X-Ray diffract-gram of the ceramic coatings, after oxidation in synthetic air, 1123 K, 50 h for: a) 97 Al_2O_3/3 TiO_2, b) 87Al_2O_3/13 TiO_2 and c) 60 Al_2O_3/40 TiO_2.

Figura 3. Espectros de difracción de los recubrimientos cerámicos después de oxidación en aire sintético a 1123 K, 50 h en: a) 97 Al_2O_3/3 TiO_2, b) 87Al_2O_3/13 TiO_2 y c) 60 Al_2O_3/40 TiO_2.

during the spraying process, and they impinge on the substrate with a high velocity, thus reducing the porosity of the coating, figure 4 a).

The 87/13 surface coating shows a greater extension of titania and lower porosity (43 %) because of titania melting, figure 4 b).

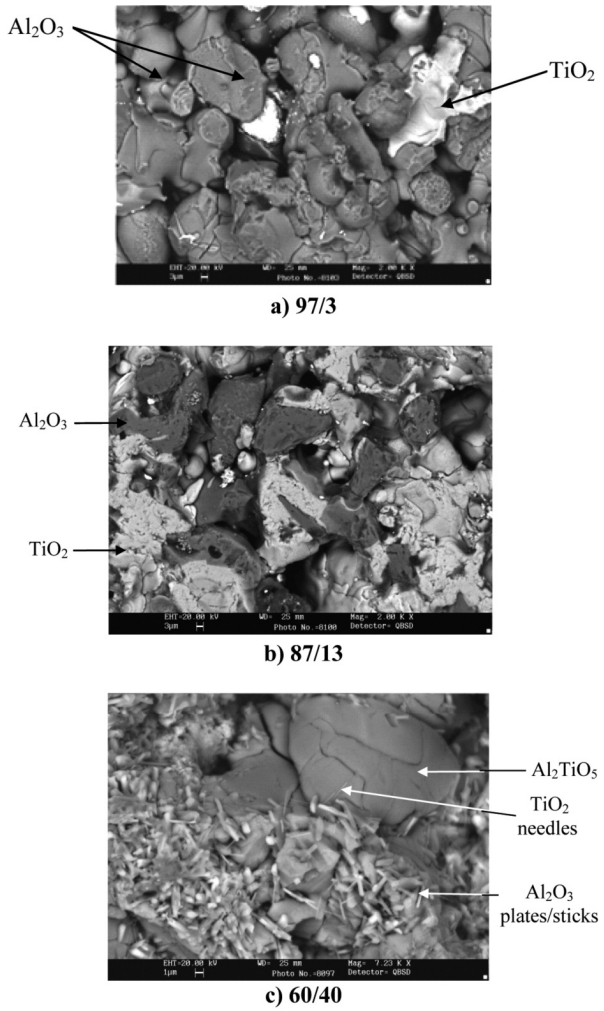

Figure 4. Superficial morphology of coatings after air oxidation at 1,123 K for 50 h: a) 97/3, particles of deformed alumina, melted titania and porosity, b) 87/13, particles of deformed alumina, melted titania and porosity and c) 60/40, Al_2TiO_5 phase, plates/sticks of α-alumina and needles of titania.

Figura 4. Morfología superficial de los recubrimientos tras oxidación en aire a 1.123 K, durante 50 h: 97/3 partículas de alúmina deformada, titania fundida y porosidad, b) 87/13 partículas de alúmina deformadas, titania fundida y porosidad y c) 60/40, fase Al_2TiO_5, placas/bastones de α-alúmia y agujas de titania.

During the oxidation process of coating 60/40, the orthorhombic Al_2TiO_5 metastable phase changes to more stable phases such as α-alumina (plates and sticks) and titania (needles), which results in a decrease in the oxidation resistance, as seen in figures 4 c), although the porosity of this layer (26 %) is lower than that of coatings 97/3 and 87/13.

The EDX microanalysis of the elements shows that the composition of each phase is close to the same value for the three ceramic coatings, as shown in table IV.

Cross-section observation

Before oxidation, EDX microanalyses indicate that the coupling layer consists of solid solution of Ni_7FeCr_2 (light grey), metallic Ni (light) and $NiAl_7O_4$ (dark), as seen in figure 5.

After oxidation, the coupling layer was partially oxidized. This occurs as a result of the inward diffusion of oxygen through the ceramic coatings. Figures 6 a), b) and c), show that the higher the TiO_2 content in the ceramic top coating, the higher the oxidation rate of the coupling layer. EDX microanalysis reveals that oxygen diffusion leads to the formation of solid solutions of Ni_8AlO_4 (dark grey) and $Ni_{10}Al_2Fe_2O$ (light), while $NiAl_7O_4$ appears during the thermal spray process and keep on stable after oxidation at 1,123 K. In addition, figures 6 a^I), b^I) and c^I) show a weak intergranular precipitation in the stainless steel base metal that was also analysed by this technique (Table V).

The mean value of the precipitated oxide depth, measured by SEM and an image analyser, depends on the titania content which also determines the oxidation rate of the coupling layer (Table VI).

We also carried out SEM examination on the specimen cross-section figure 7, in order to identify the elements incorporated during the oxidation process.

4. DISCUSSION

It was confirmed that the relation between weight gain and oxidation time obeyed the parabolic law. Equation (1) evidences that the isothermal rate constant of the parabolic curve, K_p, has a larger order of magnitude for ceramic coatings compared to AISI 304. The mass gain is principally due to the oxidation of the bounding layer and to a very little extension of precipitate in the base metal. The mass gain analysis shows the harmful effects of titania content in spite of the porosity reduction.

Table IV. Cross-section EDX microanalysis of 97/3, 87/13 and 60/40 ceramic top coatings layer, air oxidation at 1,123 K for 50 h

Tabla IV. Microanálisis EDX en la sección transversal de recubrimientos cerámicos 97/3, 87/13 y 60/40, tras oxidación en aire a 1.123 K durante 50 h

	97/3			87/13			60/40			
Elements	**Al_2O_3 %wt**	**TiO_2 %wt**	**(Ni,Fe)O %wt**	**Al_2O_3 %wt**	**TiO_2 %wt**	**(Ni,Fe)O %wt**	**Al_2TiO_5 %wt**	**Al_2O_3 %wt**	**TiO_2 %wt**	**(Ni,Fe)O %wt**
Al	54.26	—	—	54.61	—	4.52	31.06	54.32	—	3.27
Ti	—	62.01	—	—	62.96	—	27.43	—	60.83	—
Ni	—	—	74.03	—	—	68.14	—	—	—	69.48
O	45.74	37.99	20.73	45.39	37.04	23.02	41.51	45.68	39.17	22.13
Fe	—	—	5.24	—	—	4.32	—	—	—	5.12

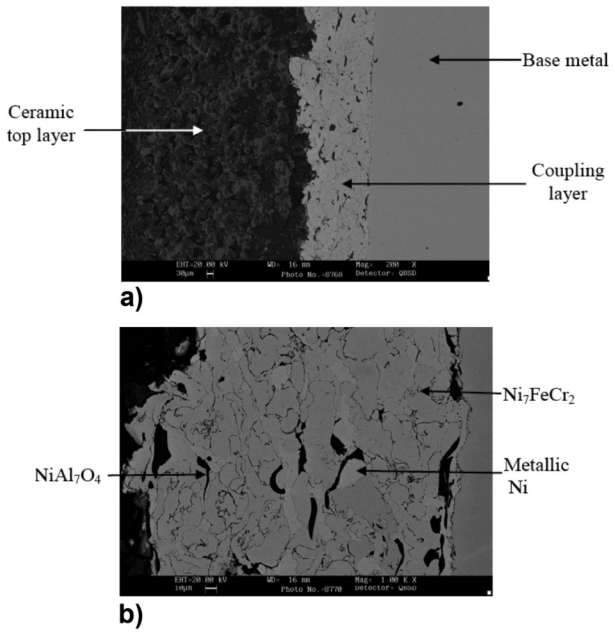

Figure 5. a) 97/3 coating before oxidation test, b) details of bonding layer phases.

Figura 5. a) Recubrimiento 97/3 antes del ensayo de oxidación, b) detalle de las fases de la capa de anclaje.

Figures 7 a^I), b^I) y c^I) show that the pores of the studied specimens are generally not connected among themselves. This might mean that titania content is the possible factor which determines the oxidation resistance losses at 1,123 K. Figures 7 a^{II}) and 7 b^{II}) show that the melting titania acts as a matrix and the plasticized alumina is enwrapped by titania. Since titania is an N-type semiconductor with a structure TiO_2-x, the x defects in the crystal lattice conduct the electrical charge. So the resistance of the titania sensors is a function of the oxygen partial pressure and the temperature[33]. Thus, the O^{-2} anion diffusivity through the titania can be considered greater than oxygen molecules diffusion throughout the unconnected pores of this type of coating.

The greater protective capacity of stainless steel without ceramic coating is due to the formation of a coherent slow-growing oxide layer (Cr_2O_3) with no spalling occurring throughout the entire test. On the other hand, SEM cross section observation shows the oxidation of Ni/Al coupling layer and base metal; this is probably due to the low contribution of the coupling layer to provide protection in this working condition.

Table V. Composition of intergranular oxidation precipitate (%)

Tabla V. Composición del precipitado de oxidación intergranular (%)

Phase	**Ni**		**Fe**		**Cr**		**O**	
	Wt	**Atom**	**Wt**	**Atom**	**Wt**	**Atom**	**Wt**	**Atom**
Fe_7Cr_7NiO	6.3	5.5	45.5	42.2	46.2	46.3	2	6

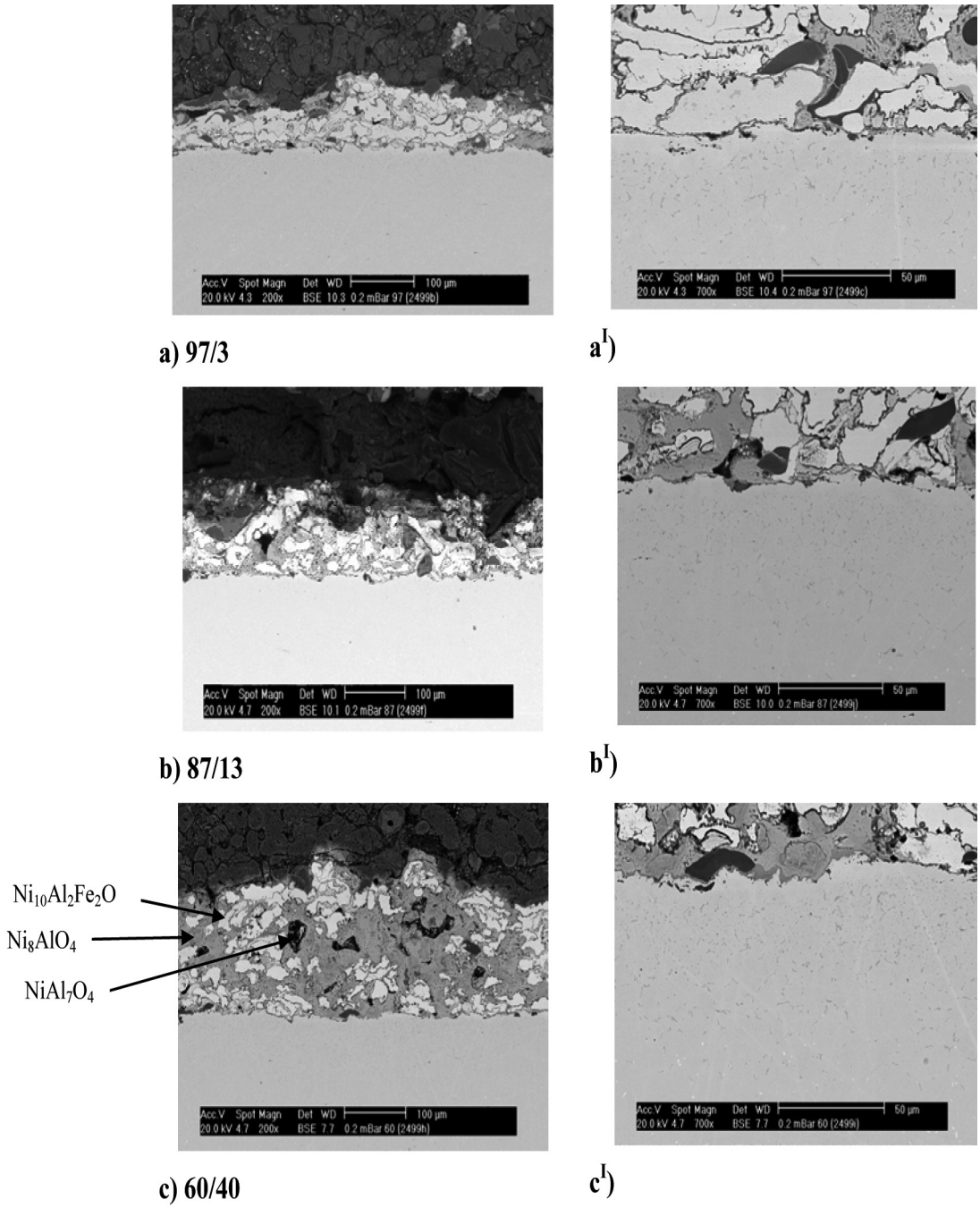

Figure 6. Cross-section of 97/3, 87/13 and 60/40 ceramic coatings oxidized at 1,123 K, for 50 h: a), b) and c) Oxidation of coupling layer and base metal, a^{I}), b^{I}) and c^{I}) intergranular oxidation of stainless steel base metal.

Figura 6. Sección transversal de los revestimientos cerámicos 97/3, 87/13 y 60/40 oxidados a 1.123 K durante 50 h: a) b) y c) Oxidación de la capa de anclaje y del metal base, a^{I}), b^{I}) y c^{I}) oxidación intergranular del acero inoxidable.

Thermal spraying of Al_2O_3/TiO_2 coatings forms metastable structures with total and partially melted regions[34-36] due to the difference in their melting points, and many microcracks and thermal stresses are generated during the cooling process.

After oxidation at 1,123 K, SEM observation of the cross-sections for the three multilayer systems showed an increase in the oxidation rate in the coupling layer as the titania content rises. Likewise, the intergranular precipitation depth in the base

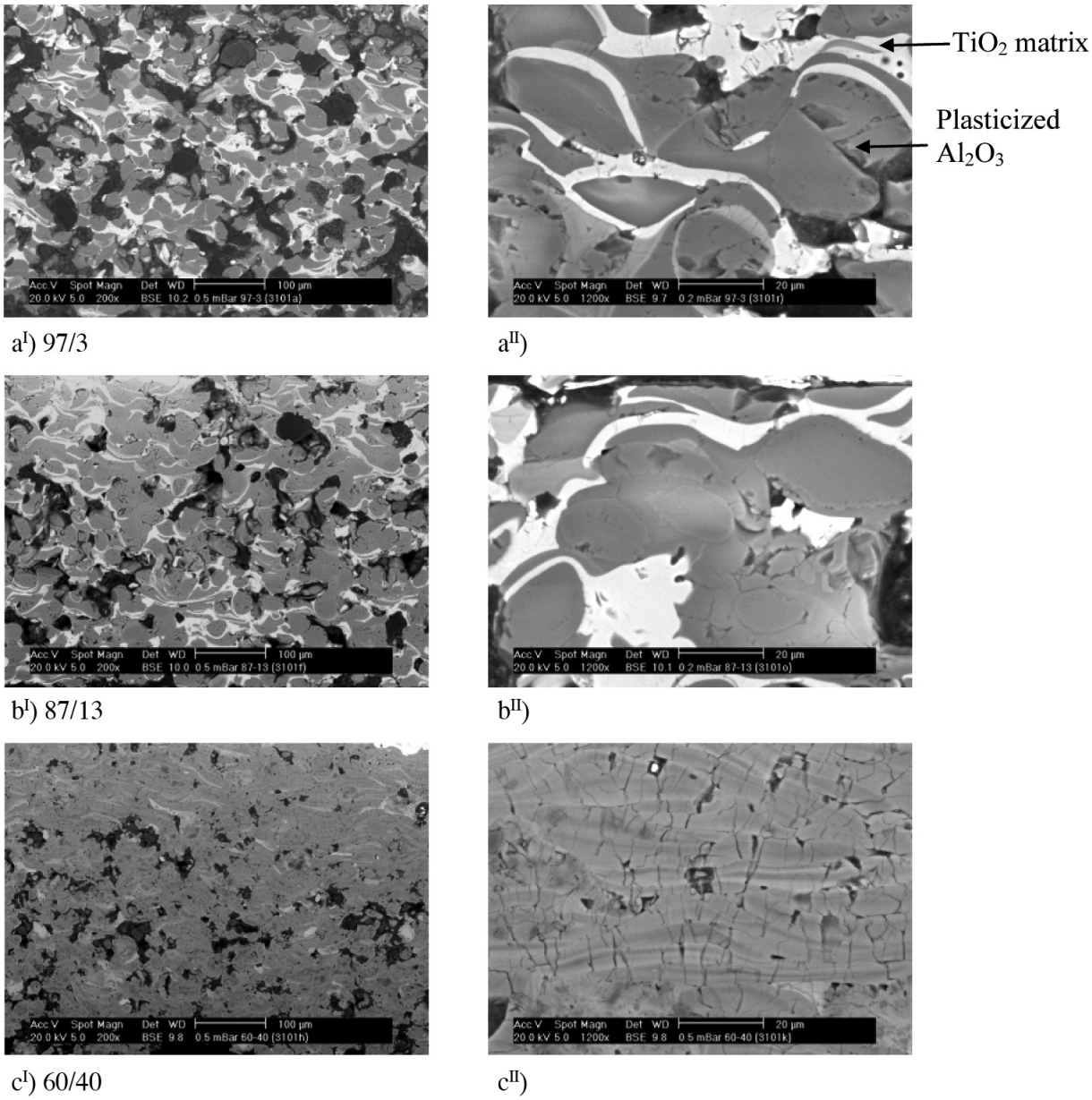

Figure 7. Cross-section, morphology and porosity: a^I) 97/3 (200x), b^I) 87/13 (200x), c^I) 60/40 (200x), a^{II}) 97/3 (1200x), b^{II}) 87/13 (1200x), c^{II}) 60/40 (1200x)

Figura 7. Morfología de la sección transversal y porosidad: a^I) 97/3 (200x), b^I) 87/13 (200x), c^I) 60/40 (200x), a^{II}) 97/3 (1200x), b^{II}) 87/13 (1200x), c^{II}) 60/40 (1200x).

metal also increases with titania percentage, so the multilayer system of top coating 97/3, with a higher alumina percentage and 53 % porosity[29], shows the best resistance to oxidation since high alumina coatings perform very well at high temperatures[31].

The 60/40 coating has the lowest alumina content and 26 % porosity. The Al_2TiO_5 metastable phase formed after the thermal spraying, partially changes to more stable phases, titania needles and alumina plates/sticks during oxidation at 1,123 K. These processes allow microstructural changes and the inward diffusion of oxygen to take place, which have severe effects of oxidation on the coupling layer and the base metal. So, the oxidation process can cause the partial equilibrium of Al_2O_3/TiO_2 coatings and the severe oxidation of 60/40 is attributed to its microstructural instability[35] and microcracking.

Since the activation energies for the diffusion processes decrease with titania content[32], the 87/13 coating, with an intermediate titania content and 43 % porosity shows an average oxidation performance.

The better oxidation resistance observed in the 97/3 and 87/13 is due to O^{-2} anion diffusion figures 7 a^{II}) and b^{II}), and the higher oxidation rates of 60/40 coating, mainly composed of Al_2TiO_5 phase, is clearly evidenced by molecular oxygen diffusion through the micro-cracking formed during oxidation process, figure 7 c^{II}).

During the thermal spray process of the bonding layer, a non-protective mixed oxide $NiAl_7O_4$ has been formed. Also the presence of Ni_7FeCr indicates that diffusion of iron and chromium from the stainless steel base metal has taken place. After oxidation at 1,123 K for 50 h other non protective phases, Ni_8AlO_4 and $Ni_{10}Al_2Fe_2O$, were obtained. Also the stainless steel base metal has not developed a protective layer and intergranular precipitation of stainless steel (Fe_7Cr_7NiO) has been detected.

It is well known that there are several ways of measuring the extent of oxidation: weight gain or loss per unit area and determination of precipitation depth. We have obtained that the quantification of coupling layer oxidation, referred to Ni_8AlO_4, is another method to evaluate the high temperature oxidation resistance of multilayer system (Table VI).

Our results showed that the oxidation behavior at 1,123 K of uncoated AISI 304 stainless steel is comparatively less affected by the temperature and time than coated with Al_2O_3/TiO_2 systems, so the application of these coatings is only required to prevent against the abrasive wear at moderated surface temperatures.

5. CONCLUSIONS

— Alumina/titania coatings containing between 3-40 % titania, deposited by the flame spray technique, hinder the protective capacity of AISI 304 stainless steel at 1,123 K, and lead to an increase of the oxidation rate in the coupling layer, thus producing intergranular precipitation (Fe and Cr oxides) in the stainless steel base metal. Top coating 60/40 exhibits higher oxidation rate than the other coatings (97/3 and 87/13) due to the high microcracking of the metastable Al_2TiO_5 phase and poor protectiveness of TiO_2.
— The maximum working temperature of this multilayer system must be well controlled to avoid the excessive oxidation rate and failure, it has been demonstrated that 1,123 K during 50 h are critical conditions for this type of coatings.
— Depth of intergranular precipitation of the base metal depends directly on the oxidation rates of the coupling layer.
— The determination of oxidation rates of Ni-Al coupling layer is a good method to evaluate the multilayer system behaviour.
— AISI 304-Ni/Al-Al_2O_3/TiO_2 system is not able to form protective oxide layers at 1,123 K which can hinder the oxidation process.
— Coatings 97/3 and 87/13 present high structural stability during thermal spraying and after 50 h of isothermal oxidation at 1,123 K, while 60/40 presents high instability after the oxidation process.

Table VI. Depth of intergranular precipitation of stainless steel base metal and coupling layer oxidation percentage

Tabla VI. Profundidad de la precipitación intergranular en el acero inoxidable y porcentaje de oxidación en la capa de anclaje

Multilayer system	Intergranular precipitation depth (μm)	Coupling layer oxidation (%)
97/3	32	22
87/13	70	50
60/40	87	86

Acknowledgments

The authors gratefully acknowledge financial support provided by Generalitat Valenciana, Conselleria De Emperesa, Universitat I Ciencia, under grants GV/2007/258. Special thanks go to Mr. J. Ortega and Ms. R. Oliver, at the Laboratory of Engineering Materials, for their help during the experiments and also to Mr. J. Gómez and Mr. G. Peris, from the SCIC at the Universitat Jaume I in Castellón.

REFERENCES

[1] K. K. de Groh, D.C. Smith, D.R. Wheeler and B.J. MacLachlan, NASA/TM-1998-208813, p. 1-10.
[2] Y. Wang, S. Jiang, M. Wang, S. Wang, T.D. Xiao, and P.R. Strutt, *Wear* 237 (2000) 176-185.
[3] J.H. Bulloch and A.G. Callagy, *Wear* 233-235 (1999) 204-292.
[4] A. Tucci and L. Esposito, *Wear* 162-164 (1993) 925-929.

[5] A. Kulkarni, S. Sampath, A. Goland and H. Herman, *Scripta Mater*. 43 (2000) 471-476.
[6] D.E. Crawmer, Handbook of Thermal Spray Technology, Ed. ASM International, Ohio, EE.UU. 2004, pp. 55-76.
[7] Y. Liu, T. E. Fischer and A. Dent, *Surf. Coat. Tech.* 167 (2003) 68-76.
[8] L. GAL-OR, I. Silberman and R. Chaim, *J. Electrochem. Soc.* 138 (1991) 1939-1941.
[9] R. Chaim, I. Silberman and L. GAL-OR, *J. Electrochem. Soc.* 138 (1991) 1942-1944.
[10] R. Chaim, G. Stark and L. Gal-Or, *J. Mater. Sci. Lett.* 13 (1994) 487-490.
[11] V.K. Tolpygo and D.R. Clarke, *Surf. Coat. Tech.* 120-121 (1999) 1-7.
[12] F.H. Sttot, G.C. Wood and J. Stringer, *Oxid. Met.* 8 (1995) 113-145.
[13] R. Zieris, S. Nowotny, L.M. Berger, L. Haubold and E. Beyer, International Thermal Spray Conference: Advancing the Science and Applying the Technology, ASM International, Orlando, EE.UU. 2003, pp. 567-577.
[14] R.S. Lima, A. Kuckuk, U. Senturk and C.C. Berndt, *J. Therm. Spray Techn.* 10 (2001) 179-185.
[15] R.S. Lima and B.R. Marple, 1st ASM International Surface Engineering Conference and the 13th IFHTSE Congress, ASM International, Columbus, OH, EE.UU., 2002, pp. 495-503.
[16] L. Dubourg, R.S. Lima and C. Moreau, *Surf. Coat. Tech.* 201 (2007) 6278-6284.
[17] R. Kossowsky and S. Singhal, Editors, *Surface Engineering, Series E: Applied Science*, Nº 85, 1984, pp. 370-389.
[18] J.A. Nesbitt, N. S. Jacobson and R.A. Miller, *Surface Modification Engineering II*, chapter 2, CRC Press, Inc., Florida, 1988, pp. 26-38.
[19] G.C. Wood, *Corr. Sci.* 2 (1962) 173-196.
[20] N. Hussain, K.A. Shahid, I.H. Khan and S. Rahman, *Oxid. Met.* 41 (1994) 215-226.
[21] Z. Kubes, J. Veselà, Z. Weiss, *J. Mater. Sci.*14 (1995) 876-877.
[22] I. Saeki, H. Konno, R. Furuichi, T. Nakamura, K. Ma buchi and M. Itoh, *Corros. Sci.* 40 (1998) 191-200.
[23] J. Botella, C. Merino and E. Otero, *Oxid. Met.* 49 (1998) 297-324.
[24] R. Guillamet, J. Lopitoux, B. Hannoyer and M. Lenglet, *Journ. Physique*, 3 (1993) 349-356.
[25] J.E. Croll and G.R. Wallwork, *Oxid. Met.* 1 (1969) 55-71.
[26] N. Karimi, F. Riffard, F. Rabaste, S. Perrier, R. Cueff, C. Issartel and H. Buscail, *Appl. Surf. Sci.* 254 (2008) 2292-2299.
[27] P.V. Ananthapadmanabhan, T.K. Thiyagarajan, K.P. Sreekumar, R.U. Satpute, N. Venkatramani and K. Ramachandran, *Surf. Coat. Tech.* 168, 2-3 (2003) 231-240.
[28] M. Wang and L.L. Shaw, *Surf. Coat. Tech.* 202 (2007) 34-44.
[29] K.H. Habib, J.J. Saura, C. Ferrer, M.S. Damra, E. Gimenez and L. Cabedo, *Surf. Coat. Tech.* 201 (2006) 1436-1443.
[30] F.J. Pérez, M.P. Hierro, F. Pedraza, M.C. Carpintero, C. Gómez and R. Tarin, *Surf. Coat. Tech.* 145 (2001) 1-7.
[31] W.J. Quadakkers, D. Naumenco, E. Wessel, V. Kochubey and L. Singheiser, *Oxid. Met.* 61 (2004) 17-37.
[32] M. Kobayashi, T. Meguro, K. Komeya, T. Yokoyama, J. Funahashi, T. Kameda, *J. Mater. Sci.* 35 (2000) 4129-4136.
[33] B. Davidov, A. Deas, O. Zagrebelny and V. Komarov, Oxygen Cell Assessment for Diving Rebreather Applications: Sourcing. Performance, Safety and Reliability. Deep Life Ltd. 2009, pp. 1-136.
[34] D. Wang, Z. Tian, L. Shen, Z. Liu and Y. Huang, *Surf. Coat. Tech.* 203 (2009) 1298-1303.
[35] L. Dubourg, R.S. Lima and C. Moreau, *Surf. Coat. Tech.* 201(2007) 6278-6284.
[36] R. Tomaszek, L. Pawlowski, J. Zdanowski, J. Grimblot and J. Laureyns, *Surf. Coat. Tech.* 185 (2004) 137-149.